

Hopf Bifurcation of a Delayed SVEIS Worm Propagation Model with Nonlinear Incidence Rate

Zizhen Zhang[1(✉)], Weishi Zhang[1], and Anwar Zeb[2]

[1] School of Management Science and Engineering, Anhui University of Finance and Economics, Bengbu 233030, China
zzzhaida@163.com

[2] Department of Mathematics, COMSATS University Islamabad, Abbottabad, Pakistan
anwar@cuiatd.edu.pk

Abstract. In the present internet age, worms pose a great threat to network security. It is urgent to explore the spreading law of worms through networks. To this end, an SVEIS(Susceptible-Vaccinated-Exposed-Infectious) worm propagation model with nonlinear incidence rate and time delay is proposed in this study. A series of sufficient conditions for local stability and appearance of Hopf bifurcation are derived through taking the time delay as bifurcation parameter. Moreover, direction and stability of the Hopf bifurcation are established with aids of center manifold method. Finally, a numerical example is demonstrated to certificate theoretical findings.

Keywords: Hopf bifurcation · Delay · SVEIS model · Nonlinear incidence rate · Stability

1 Introduction

The advent of the internet age has given rise to enormous changes in modern society. For example, we can easily access data and information by simply clicking a button, and we can buy what we need without leaving home. However, in the meantime, the rapid development of internet technologies has brought about severe challenges for safeguarding the valuable data or information stored in computers and for the data or information in transit [1]. Worms act like communicable diseases and they are epidemic in nature. Therefore, it is possible to establish mathematical models to represent the behavior of a computer worm, which is a self contained program. In fact, there have been some works about mathematical models for worm propagation in networks. Feng et al. [2] formulated an SIRS(Susceptible-Infectious-Recovered-Susceptible) worm propagation model in wireless sensor network. Nevertheless, one of the significant characteristics of

Supported by Anhui University of Finance and Economics.

© The Author(s), under exclusive license to Springer Nature Switzerland AG 2023
O. Gervasi et al. (Eds.): ICCSA 2023 Workshops, LNCS 14104, pp. 130–143, 2023.
https://doi.org/10.1007/978-3-031-37105-9_10

worms such as the Code Red worm [3] and the Witty worm [4] is their incubation. In another word, when a worm enters into a susceptible computer, it hides itself and becomes infectious after a period. From this point of view, the SIRS model [2] ignores the incubation period during the propagation process of computer worms. Due to this fact, Hosseini et al. [5–7] formulated and investigated different forms of SEIRS(Susceptible-Exposed-Infectious-Recovered-Susceptible) worm propagation model. Considering the effect of quarantine, some scholars have proposed and analyzed some worm propagation models including quarantine [8–10].

Vaccination is proverbially thought of one of the most significant measures to struggle against the propagation of computer viruses in networks. Some mathematical models on the propagation of worms have been developed [11–14]. Nevertheless, the aforementioned models include vaccination strategy on the basis of the bilinear incidence rate, which is suitable just for the situation when the fraction of the infected computers is not large. With the popular use of networks in our daily life, the number of infected computers in networks maybe large in real network world. To overcome the defect of the bilinear incidence rate, Upadhyay and Kumari [15] established the following worm propagation model incorporating nonlinear incidence rate and vaccination:

$$\begin{cases} \frac{dS(t)}{dt} = \Lambda - \mu S(t) - \omega S(t) + \theta V(t) - \frac{\beta S(t) I(t)}{S(t)+I(t)+c} + (1-q)\gamma I(t), \\ \frac{dV(t)}{dt} = \omega S(t) - \theta V(t) - \mu V(t) + \xi E(t) + q\gamma I(t), \\ \frac{dE(t)}{dt} = \frac{\beta S(t) I(t)}{S(t)+I(t)+c} - \mu E(t) - \xi E(t) - \sigma E(t), \\ \frac{dI(t)}{dt} = \sigma E(t) - \mu I(t) - \gamma I(t), \end{cases} \tag{1}$$

where $S(t)$, $V(t)$, $E(t)$ and $I(t)$ denote the numbers of the susceptible nodes, the vaccinated nodes, the exposed nodes and the infectious nodes, separately. Λ is the constant recruitment rate of the susceptible nodes; μ is the crashing rate of all the nodes; β is the contact rate between the susceptible and the infectious nodes; c is the half saturation constant and q is the proportion of recovered nodes gaining worm-acquired immunity. ω, θ, ξ, σ and γ are the state transition probabilities. Upadhyay and Kumari [15] examined stability analysis of the model system (1).

Actually, dynamics of mathematical models not only implicate stability, but also include bifurcation and periodic phenomenon [16]. Although the law of motion of a system is related to the state of motion at the present moment, it can also be influenced by the state of motion at some moments or some moments in the past. Time delay phenomenon is a kind of physical phenomenon that exists widely in the actual engineering control process. Considering the effect of time delay in the mathematical model would be more relevant to real life. Particularly, differential equations incorporating time delays experience much more tanglesome dynamical behaviors compared to ordinary differential equations. Consequently, we shall explore the Hopf bifurcation induced by time delay because of incubation period of worms into the model system (1) and consider the delayed worm propagation model described in the following form:

$$\begin{cases} \frac{dS(t)}{dt} = \Lambda - \mu S(t) - \omega S(t) + \theta V(t) - \frac{\beta S(t) I(t)}{S(t)+I(t)+c} + (1-q)\gamma I(t), \\ \frac{dV(t)}{dt} = \omega S(t) - \theta V(t) - \mu V(t) + \xi E(t) + q\gamma I(t), \\ \frac{dE(t)}{dt} = \frac{\beta S(t) I(t)}{S(t)+I(t)+c} - \mu E(t) - \xi E(t) - \sigma E(t-\tau), \\ \frac{dI(t)}{dt} = \sigma E(t-\tau) - \mu I(t) - \gamma I(t), \end{cases} \tag{2}$$

in which τ is the time delay because of incubation period of worms.

The skeleton of this study is as follows. Local stability and Hopf bifurcation is analyzed and crucial point of the time delay at which a Hopf bifurcation appear is determined in the next section. Direction and stability of the Hopf bifurcation are determined in Sect. 3. A numerical example is presented to certificate the correctness of the analytical findings in Sect. 4. Section 5 concludes our study.

2 Analysis of Local Stability and Hopf Bifurcation

On the basis of the calculation by Upadhyay and Kumari [15], it can be concluded that if the basic reproduction number $R_0 = \frac{\Lambda\beta\sigma(\mu+\theta)}{\kappa_2(\mu+\gamma)(\Lambda(\mu+\theta)+c\mu\kappa_1)} > 1$ where $\kappa_1 = \mu + \theta + \omega$ and $\kappa_2 = \mu + \xi + \sigma$, then the model system (2) exists an unique endemic equilibrium $W_*(S_*, V_*, E_*, I_*)$, where

$$\begin{aligned} S_* &= \frac{I_* + c}{\Delta_1}, E_* = \frac{(\mu+\gamma) I_*}{\sigma}, \\ V_* &= \frac{(\omega + \Delta_1\Delta_2) I_* + c\omega}{\Delta_1(\mu+\theta)}, \\ I_* &= \frac{\sigma\Lambda\Delta_1(\mu+\theta) - c\mu\sigma\kappa_1}{\mu(\Delta_1\Delta_3 + \sigma\kappa_1)}, \end{aligned}$$

with

$$\begin{aligned} \Delta_1 &= R_0 - 1 + \frac{cR_0}{S^0}, \\ \Delta_2 &= \frac{\xi(\mu+\gamma)}{\sigma} + q\gamma, \\ \Delta_3 &= (\mu+\gamma)(\mu+\xi+\theta) + \sigma(\mu+q\gamma+\theta), \\ S^0 &= \frac{\Lambda(\mu+\theta)}{\mu\kappa_1}. \end{aligned} \tag{3}$$

The Jacobian matrix Q_* at $W_*(S_*, V_*, E_*, I_*)$ is presented by

$$Q_* = \begin{bmatrix} k_{11} & k_{12} & 0 & k_{14} \\ k_{21} & k_{22} & k_{23} & k_{24} \\ k_{31} & 0 & k_{33} + l_{33}e^{-\lambda\tau} & k_{34} \\ 0 & 0 & l_{43}e^{-\lambda\tau} & k_{44} \end{bmatrix}, \tag{4}$$

where

$$
\begin{aligned}
k_{11} &= -\mu - \omega - \frac{\beta I_*(I_* + c)}{(S_* + I_* + c)^2}, k_{12} = \theta, \\
k_{14} &= (1-q)\gamma - \frac{\beta S_*(S_* + c)}{(S_* + I_* + c)^2}, \\
k_{21} &= \omega, k_{22} = -\mu - \theta, k_{23} = \xi, k_{24} = q\gamma, \\
k_{31} &= \frac{\beta I_*(I_* + c)}{(S_* + I_* + c)^2}, k_{33} = -\mu - \xi, \\
k_{34} &= \frac{\beta S_*(S_* + c)}{(S_* + I_* + c)^2}, l_{33} = -\sigma, \\
k_{44} &= -\mu - \gamma, l_{43} = \sigma.
\end{aligned}
$$

The characteristic equation of Jacobian matrix W_* can be obtained with

$$\lambda^4 + \Theta_3\lambda^3 + \Theta_2\lambda^2 + \Theta_1\lambda + \Theta_0 + (\Delta_3\lambda^3 + \Delta_2\lambda^2 + \Delta_1\lambda + \Delta_0)e^{-\lambda\tau} = 0, \quad (5)$$

with

$$
\begin{aligned}
\Theta_0 &= k_{33}k_{44}(k_{11}k_{22} - k_{12}k_{21}), \\
\Theta_1 &= k_{12}k_{21}(k_{33} + k_{44}) - k_{11}k_{33}(k_{22} + k_{44}) - k_{22}k_{44}(k_{11} + k_{33}), \\
\Theta_2 &= k_{11}k_{33} + k_{22}k_{44} - k_{12}k_{21} + (k_{11} + k_{33})(k_{22} + k_{44}), \\
\Theta_3 &= -(k_{11} + k_{22} + k_{33} + k_{44}), \\
\Delta_0 &= k_{44}l_{33}(k_{11}k_{12} - k_{12}k_{21}) + k_{12}l_{43}(k_{21}k_{34} - k_{24}k_{31}) + k_{22}l_{43}(k_{31}k_{14} - k_{34}k_{11}), \\
\Delta_1 &= k_{12}k_{21}l_{33} - k_{14}k_{31}l_{43} + k_{34}l_{43}(k_{11} + k_{22}) - l_{33}(k_{11}k_{22} + k_{11}k_{44} + k_{22}k_{44}), \\
\Delta_2 &= l_{33}(k_{11} + k_{22} + k_{44}) - l_{34}l_{43}, \Delta_3 = -l_{33}.
\end{aligned}
$$

Lemma 1 [16]**.** $W_*(S_*, V_*, E_*, I_*)$ is locally asymptotically stable if $\sigma\beta(S_* + c)S_* \leq \kappa_2(\mu + \gamma)(S_* + I_* + c)^2$ is satisfied when $\tau = 0$.

For $\tau > 0$, assume that $\lambda = i\upsilon(\upsilon > 0)$ is a root of Eq. (5). Thus

$$
\begin{cases}
(\Delta_1\upsilon - \Delta_3\upsilon^3)\sin(\tau\upsilon) + (\Delta_0 - \Delta_2\upsilon^2)\cos(\tau\upsilon) = \Theta_2\upsilon^2 - \upsilon^4 - \Theta_0, \\
(\Delta_1\upsilon - \Delta_3\upsilon^3)\cos(\tau\upsilon) - (\Delta_0 - \Delta_2\upsilon^2)\sin(\tau\upsilon) = \Theta^3\upsilon^3 - \Theta_1\upsilon,
\end{cases} \quad (6)
$$

leading to

$$\upsilon^8 + \Upsilon_3\upsilon^6 + \Upsilon_2\upsilon^4 + \Upsilon_1\upsilon^2 + \Upsilon_0 = 0, \quad (7)$$

where

$$
\begin{aligned}
\Upsilon_0 &= \Theta_0^2 - \Delta_0^2, \\
\Upsilon_1 &= \Theta_1^2 - \Delta_1^2 + 2\Delta_0\Delta_2 - 2\Theta_0\Theta_2, \\
\Upsilon_2 &= \Theta_2^2 - \Delta_2^2 + 2\Delta_1\Delta_3 + 2\Theta_1\Theta_3 - 2\Theta_0, \\
\Upsilon_3 &= \Theta_3^2 - \Delta_3^2 - 2\Theta_2.
\end{aligned}
$$

Define $\upsilon^2 = \varpi$. Equation (7) equals

$$\varpi^4 + \Upsilon_3\varpi^3 + \Upsilon_2\varpi^2 + \Upsilon_1\varpi + \Upsilon_0 = 0. \quad (8)$$

Discussion regarding the distribution of roots for Eq. (8) is similar to that analyzed by Li and Wei [17]. For the mathematical convenience, we suppose that Eq. (8) exists at least one ϖ_0 ($\varpi_0 > 0$) and moreover, Eq. (7) exists $\upsilon_0 = \sqrt{\varpi_0}$ leading to that Eq. (5) has a pair of purely imaginary roots $\pm i\upsilon_0$. From Eq. (6), one has

$$\tau_i = \frac{1}{\upsilon_0} \arccos[\frac{P_1(\upsilon_0)}{P_2(\upsilon_0)}] + \frac{2i\pi}{\upsilon_0}, \tag{9}$$

with

$$\begin{aligned} P_1(\upsilon_0) &= (\Delta_2 - \Delta_3\Theta_3)\upsilon_0^6 + (\Delta_1\Theta_3 + \Delta_3\Theta_1 - \Delta_0 - \Delta_2\Theta_2)\upsilon_0^4 \\ &\quad +(\Delta_0\Theta_2 + \Delta_2\Theta_0 - \Delta_1\Theta_1)\upsilon_0^2 - \Delta_0\Theta_0, \\ P_2(\upsilon_0) &= \Delta_3^2\upsilon_0^6 + (\Delta_2^2 - 2\Delta_1\Delta_3)\upsilon_0^4 + (\Delta_1^2 - 2\Delta_0\Delta_2)\upsilon_0^2 + \Delta_0^2. \end{aligned}$$

Let

$$\tau_0 = min\{\tau_i\}, i = 0, 1, 2, \cdots. \tag{10}$$

Based on Eq. (5), one has

$$[\frac{d\lambda}{d\tau}]^{-1} = -\frac{P_3(\lambda)}{P_4(\lambda)} + \frac{P_5(\lambda)}{P_6(\lambda)} - \frac{\tau}{\lambda}, \tag{11}$$

where

$$\begin{aligned} P_3(\lambda) &= 4\lambda^3 + 3\Theta_3\lambda^2 + 2\Theta_2\lambda + \Theta_1, \\ P_4(\lambda) &= \lambda^5 + \Theta_3\lambda^4 + \Theta_2\lambda^3 + \Theta_1\lambda^2 + \Theta_0\lambda, \\ P_5(\lambda) &= 3\Delta_3\lambda^2 + 2\Delta_2\lambda + \Delta_1, \\ P_6(\lambda) &= \Delta_3\lambda^4 + \Delta_2\lambda^3 + \Delta_1\lambda^2 + \Delta_0\lambda. \end{aligned}$$

This gives

$$Re[\frac{d\lambda}{d\tau}]^{-1}_{\lambda=i\upsilon_0} = \frac{Q'(\varpi_0)}{P_2(\upsilon_0)}, \tag{12}$$

where $Q(\varpi) = \varpi^4 + \Upsilon_3\varpi^3 + \Upsilon_2\varpi^2 + \Upsilon_1\varpi + \Upsilon_0$ and $\varpi_0 = \upsilon_0^2$. Clearly, if $Q'(\varpi_0) \neq 0$, in accordance withs of the Hopf bifurcation theorem proposed by Hassard et al. in [18], we can stated the obtained results in the following theorem.

Theorem 1. *If $R_0 > 1$, then endemic equilibrium $W_*(S_*, V_*, E_*, I_*)$ is locally asymptotically stable whenever $\tau \in [0, \tau_0)$; while a Hopf bifurcation experiences near $W_*(S_*, V_*, E_*, I_*)$ when $\tau = \tau_0$ and a cluster of periodic solutions exhibit around $W_*(S_*, V_*, E_*, I_*)$.*

3 Direction and Stability of the Hopf Bifurcation

In this section, we derive the explicit formula governing direction and stability of the Hopf bifurcation exhibits at $W_*(S_*, V_*, E_*, I_*)$ when $\tau = \tau_0$. Denote $\sigma = \tau + \tau_0$, $\sigma \in \Re$, $t = s\tau$, $S(s\tau) = S(s)$, $V(s\tau) = V(s)$, $E(s\tau) = E(s)$, $I(s\tau) = I(s)$.

Define $X_1(t) = S(t) - S_*$, $X_2(t) = V(t) - V_*$, $X_3(t) = E(t) - E_*$ and $X_4 = I(t) - I_*$, then the model system (2) is equivalent to

$$\dot{X}(t) = L_\sigma(X_t) + F(\sigma, X_t), \tag{13}$$

where $X(t) = (X_1(t), X_2(t), X_3(t), X_4(t))^T \in C = C([-1, 0], \Re^3)$, $X_t(\vartheta) = X(t+\vartheta) = (X_1(t+\vartheta), X_2(t+\vartheta), X_3(t+\vartheta), X_4(t+\vartheta))^T \in C$ and $L_\sigma : C \to \Re^4$, $F : \Re \times C \to \Re^4$ are

$$L_\sigma(\varsigma) = (\sigma + \tau_0)[K\varsigma(0) + L\varsigma(-1)], \tag{14}$$

and

$$F(\sigma, \varsigma) = (\sigma + \tau_0)(F_1, 0, F_3, 0)^T, \tag{15}$$

where

$$K = \begin{pmatrix} k_{11} & k_{12} & 0 & k_{14} \\ k_{21} & k_{22} & k_{23} & k_{24} \\ k_{31} & 0 & k_{33} & k_{34} \\ 0 & 0 & 0 & k_{44} \end{pmatrix}, L = \begin{pmatrix} 0 & 0 & 0 & 0 \\ 0 & 0 & 0 & 0 \\ 0 & 0 & l_{33} & 0 \\ 0 & 0 & l_{43} & 0 \end{pmatrix},$$

and

$$\begin{aligned} F_1 &= k_{15}\varsigma_1^2(0) + k_{16}\varsigma_1(0)\varsigma_3(0) + k_{17}\varsigma_3^2(0) + k_{18}\varsigma_1^2(0)\varsigma_3(0) \\ &\quad + \varsigma_{19}\varsigma_1(0)\varsigma_2^2(0) + k_{110}\varsigma_1^3(0) + k_{111}\varsigma_2^3(0) + \cdots, \\ F_3 &= k_{35}\varsigma_1^2(0) + k_{36}\varsigma_1(0)\varsigma_3(0) + k_{37}\varsigma_3^2(0) + k_{38}\varsigma_1^2(0)\varsigma_3(0) \\ &\quad + \varsigma_{39}\varsigma_1(0)\varsigma_2^2(0) + k_{310}\varsigma_1^3(0) + k_{311}\varsigma_2^3(0) + \cdots, \end{aligned}$$

where

$$\begin{aligned} k_{15} &= \frac{\beta I_*(I_* + c)}{(S_* + I_* + c)^3}, k_{16} = -\frac{2\beta S_* I_* + c\beta(S_* + I_* + c)}{(S_* + I_* + c)^3}, \\ k_{17} &= \frac{\beta S_*(S_* + c)}{(S_* + I_* + c)^3}, k_{18} = \frac{6\beta S_* I_* + c\beta(S_* + I_* + c) - \beta I_*(I_* + c)}{(S_* + I_* + c)^4}, \\ k_{19} &= \frac{6\beta S_* I_* + c\beta(S_* + I_* + c) - \beta S_*(S_* + c)}{(S_* + I_* + c)^4}, \\ k_{110} &= -\frac{\beta I_*(I_* + c)}{(S_* + I_* + c)^4}, k_{111} = \frac{\beta S_*(S_* + c)}{(S_* + I_* + c)^4}, \\ k_{35} &= -k_{15}, k_{36} = -k_{16}, k_{37} = -k_{17}, k_{38} = -k_{18}, \\ k_{39} &= -k_{19}, k_{310} = -k_{110}, k_{311} = -k_{111}. \end{aligned}$$

Thus, there exists $\eta(\varsigma, \sigma)$ for $\sigma \in [-1, 0]$ satisfying

$$L_\sigma(\phi) = \int_{-1}^{0} d\eta(\varsigma, \sigma)\phi(\varsigma). \tag{16}$$

Define

$$\eta(\varsigma, \sigma) = (\tau_0 + \sigma)(K\delta(\varsigma) + L\delta(\varsigma + 1)). \tag{17}$$

For $\phi \in C([-1,0],\Re^4)$,

$$A(\sigma)\phi = \begin{cases} \frac{d\phi(\varsigma)}{d\varsigma}, & -1 \le \varsigma < 0, \\ \int_{-1}^{0} d\eta(\varsigma,\sigma)\phi(\varsigma), & \varsigma = 0, \end{cases} \tag{18}$$

and

$$R(\sigma)\phi = \begin{cases} 0, & -1 \le \varsigma < 0, \\ F(\sigma,\phi), & \varsigma = 0, \end{cases} \tag{19}$$

Then system (13) becomes

$$\dot{X}(t) = A(\sigma)X_t + R(\sigma)X_t. \tag{20}$$

For $\varphi \in C^1([0,1],(\Re^4)^*)$,

$$A^*(\varphi) = \begin{cases} -\frac{d\varphi(s)}{ds}, & 0 < s \le 1, \\ \int_{-1}^{0} d\eta^T(s,0)\varphi(-s), & s = 0 \end{cases} \tag{21}$$

and

$$\langle \varphi(s), \phi(\varsigma)\rangle = \bar{\varphi}(0)\phi(0) - \int_{\varsigma=-1}^{0}\int_{\rho=0}^{\varsigma} \bar{\varphi}(\rho-\varsigma)d\eta(\varsigma)\phi(\rho)d\rho. \tag{22}$$

Suppose that the eigenvector $\Psi(\varsigma) = (1,\Psi_2,\Psi_3,\Psi_4)^T e^{i\upsilon_0\tau_0\varsigma}$ of $A(0)$ related to $+i\upsilon_0\tau_0$ and the eigenvector $\Psi^*(\varsigma) = M(1,\Psi_2^*,\Psi_3^*,\Psi_4^*)e^{i\upsilon_0\tau_0 s}$ of $A^*(0)$ related to $-i\upsilon_0\tau_0$. Then it is not difficult to validate that

$$\begin{aligned}
\Psi_2 &= \frac{i\upsilon_0 - k_{11} - k_{14}\Psi_4}{k_{12}}, \\
\Psi_3 &= \frac{i\upsilon_0 - k_{34}}{(i\upsilon_0 - k_{34})(i\upsilon_0 - k_{33} - l_{33}e^{-i\tau_0\upsilon_0}) - k_{34}l_{43}e^{-i\tau_0\upsilon_0}}, \\
\Psi_4 &= \frac{l_{43}e^{-i\tau_0\upsilon_0}\Psi_3}{i\upsilon_0 - k_{44}}, \\
\Psi_2^* &= -\frac{k_{12}}{i\upsilon_0 + k_{22}}, \\
\Psi_3^* &= \frac{k_{12}k_{21}}{k_{31}(i\upsilon_0 + k_{22})} - (i\upsilon_0 + k_{11}), \\
\Psi_4^* &= -\frac{k_{23}\Psi_2^* + (i\upsilon_0 + k_{33} + l_{33}e^{i\upsilon_0\tau_0})\Psi_3^*}{l_{43}e^{i\upsilon_0\tau_0}}.
\end{aligned}$$

and

$$\langle \Psi^*, \Psi\rangle = 1, \langle \Psi^*, \bar{\Psi}\rangle = 0,$$

where

$$M = \frac{1}{1 + \Psi_2\bar{\Psi}_2^* + \Psi_3\bar{\Psi}_3^* + \Psi_4\bar{\Psi}_4^* + \Psi_3 e^{-i\upsilon_0\tau_0}(l_{33}\bar{\Psi}_3^* + l_{43}\bar{\Psi}_4^*)}.$$

The detailed expressions of coefficients w_{20}, w_{11}, w_{02} and w_{21} can be determined on the basis of the calculation process in [18]:

$$
\begin{aligned}
w_{20} &= 2\bar{M}\tau_0[k_{15}+k_{16}\Psi_3+k_{17}\Psi_3^2+\bar{\Psi}_3^*(k_{35}+k_{36}\Psi_3+k_{37}\Psi_3^2)],\\
w_{11} &= \bar{M}\tau_0[2k_{15}+k_{16}(\bar{\Psi}_3+\Psi_3)+2k_{17}\bar{\Psi}_3\Psi_3+\bar{\Psi}_3^*(2k_{35}+k_{36}(\bar{\Psi}_3+\Psi_3)+2k_{37}\bar{\Psi}_3\Psi_3)],\\
w_{02} &= 2\bar{M}\tau_0[k_{15}+k_{16}\bar{\Psi}_3+k_{17}\bar{\Psi}_3^2+\bar{\Psi}_3^*(k_{35}+k_{36}\bar{\Psi}_3+k_{37}\bar{\Psi}_3^2)],\\
w_{21} &= 2\bar{M}\tau_0[k_{15}(2B_{11}^{(1)}(0)+B_{20}^{(1)}(0))+k_{16}(B_{11}^{(1)}(0)\Psi_3+\frac{1}{2}B_{20}^{(1)}(0)\bar{\Psi}_3+B_{11}^{(3)}(0)+\frac{1}{2}B_{20}^{(3)}(0))\\
&\quad +k_{17}(2B_{11}^{(3)}(0)+B_{20}^{(3)}(0))+k_{18}(\bar{\Psi}_3^2+2\Psi_3)+k_{19}(\Psi_3^2+2\Psi_3\bar{\Psi}_3)+3k_{110}+3k_{111}\Psi_3^2\bar{\Psi}_3\\
&\quad +\bar{\Psi}_3^*(k_{35}(2B_{11}^{(1)}(0)+B_{20}^{(1)}(0))+k_{36}(B_{11}^{(1)}(0)\Psi_3+\frac{1}{2}B_{20}^{(1)}(0)\bar{\Psi}_3+B_{11}^{(3)}(0)+\frac{1}{2}B_{20}^{(3)}(0))\\
&\quad +k_{37}(2B_{11}^{(3)}(0)+B_{20}^{(3)}(0))+k_{38}(\bar{\Psi}_3^2+2\Psi_3)+k_{39}(\Psi_3^2+2\Psi_3\bar{\Psi}_3)+3k_{310}+3k_{311}\Psi_3^2\bar{\Psi}_3)],
\end{aligned}
$$

with

$$B_{20}(\varsigma)=\frac{iw_{20}}{\upsilon_0\tau_0}\Psi(\varsigma)+\frac{i\bar{w}_{02}}{3\upsilon_0\tau_0}\bar{\Psi}(\varsigma)+\Omega_1 e^{2i\upsilon_0\tau_0\varsigma}, \tag{23}$$

$$B_{11}(\varsigma)=-\frac{iw_{11}}{\upsilon_0\tau_0}\Psi(\varsigma)+\frac{i\bar{w}_{11}}{\upsilon_0\tau_0}\bar{\Psi}(\varsigma)+\Omega_2, \tag{24}$$

where

$$\begin{pmatrix} 2i\upsilon_0-k_{11} & -k_{12} & 0 & -k_{14}\\ -k_{21} & 2i\upsilon_0-k_{22} & -k_{23} & -k_{24}\\ -k_{31} & 0 & 2i\upsilon_0-k_{33}-l_{33}e^{-2i\upsilon_0\tau_0} & -k_{34}\\ 0 & 0 & -l_{43}e^{-2i\upsilon_0\tau_0} & -k_{44}\end{pmatrix}\Omega_1=\begin{pmatrix}\Omega_{11}\\0\\\Omega_{13}\\0\end{pmatrix}, \tag{25}$$

$$\begin{pmatrix} k_{11} & k_{12} & 0 & k_{14}\\ k_{21} & k_{22} & k_{23} & k_{24}\\ k_{31} & 0 & k_{33}+l_{33} & k_{34}\\ 0 & 0 & l_{43} & k_{44}\end{pmatrix}\Omega_2=\begin{pmatrix}\Omega_{31}\\0\\\Omega_{33}\\0\end{pmatrix}, \tag{26}$$

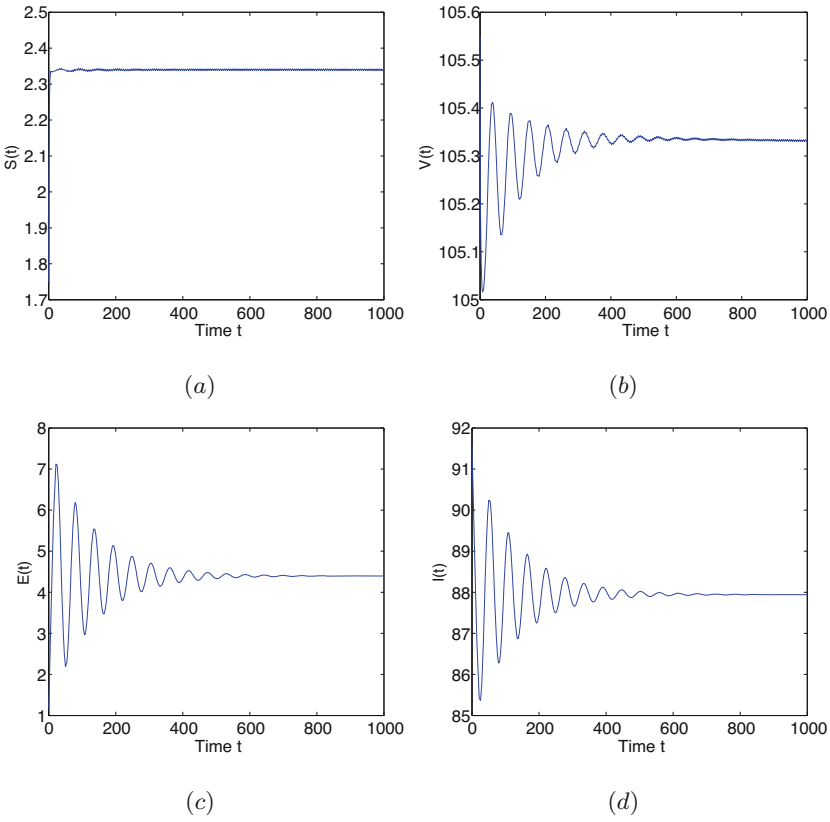
where

$$
\begin{aligned}
\Omega_{11} &= k_{15}+k_{16}\Psi_3+k_{17}\Psi_3^2,\\
\Omega_{13} &= k_{35}+k_{36}\Psi_3+k_{37}\Psi_3^2,\\
\Omega_{31} &= 2k_{15}+k_{16}(\bar{\Psi}_3+\Psi_3)+2k_{17}\bar{\Psi}_3\Psi_3,\\
\Omega_{33} &= 2k_{35}+k_{36}(\bar{\Psi}_3+\Psi_3)+2k_{37}\bar{\Psi}_3\Psi_3.
\end{aligned}
$$

Thus, we have

$$
\begin{aligned}
C_1(0) &= \tfrac{i}{2\upsilon_0\tau_0}\left(w_{11}w_{20}-2|w_{11}|^2-\tfrac{|w_{02}|^2}{3}\right)+\tfrac{w_{21}}{2}\\
\Pi_0 &= -\tfrac{Re\{C_1(0)\}}{Re\{\lambda'(\tau_0)\}},\\
\Pi_1 &= 2Re\{C_1(0)\}.
\end{aligned} \tag{27}
$$

Theorem 2. The Hopf bifurcation at $\tau = \tau_0$ is supercritical (subcritical) if $\Pi_0 > 0$ ($\Pi_0 < 0$); The periodic solutions exhibiting around the endemic equilibrium point $W_*(S_*, V_*, E_*, I_*)$ is stable (unstable) if $\Pi_1 < 0$ ($\Pi_1 > 0$).

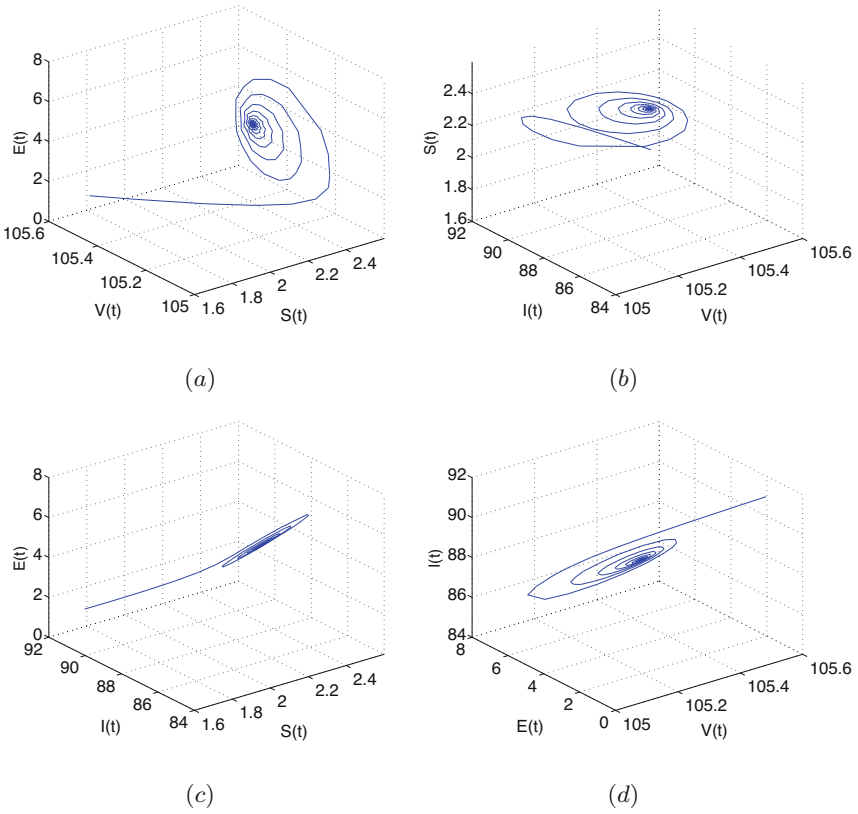


(a) (b) (c) (d)

Fig. 1. The time plots for $\tau = 14.4705 < \tau_0 = 15.6626$.

4 Numerical Simulations

In the current section, we utilize the numerical simulations to verify the obtained analytical results in Sect. 2 and Sect. 3. The parameter values are fixed as follows: Choosing $\Lambda = 0.4$, $\mu = 0.002$, $\theta = 0.014$, $\omega = 0.6$, $\beta = 0.24$, $c = 10$, $q = 0.9$, $\gamma = 0.003$, $\xi = 0.01$, $\sigma = 0.1$. Then the model system (2) becomes



(a) (b) (c) (d)

Fig. 2. The phase plots for $\tau = 14.4705 < \tau_0 = 15.6626$.

$$\begin{cases} \frac{dS(t)}{dt} = 0.4 - 0.602\,S(t) + 0.014\,V(t) - \frac{0.24\,S(t)I(t)}{S(t)+I(t)+10} + 0.0003I(t), \\ \frac{dV(t)}{dt} = 0.6\,S(t) - 0.016\,V(t) + 0.01E(t) + 0.0027I(t), \\ \frac{dE(t)}{dt} = \frac{0.24\,S(t)I(t)}{S(t)+I(t)+10} - 0.012E(t) - 0.1E(t-\tau), \\ \frac{dI(t)}{dt} = 0.1E(t-\tau) - 0.005I(t), \end{cases} \tag{28}$$

from which one has $R_0 = 14.6520 > 1$ and then the unique endemic equilibrium point $W_*(2.3398, 105.3279, 4.3968, 87.9355)$ is obtained. By calculations, we obtain $\sigma\beta(S_* + c)S_* = 0.6929$ and $\kappa_2(\mu + \gamma)(S_* + I_* + c)^2 = 5.6309$. Thus, $\sigma\beta(S_* + c)S_* \leq \kappa_2(\mu + \gamma)(S_* + I_* + c)^2$ is satisfied. Accordingly, we can know that the model system (28) is locally asymptotically stable whenever $\tau = 0$.

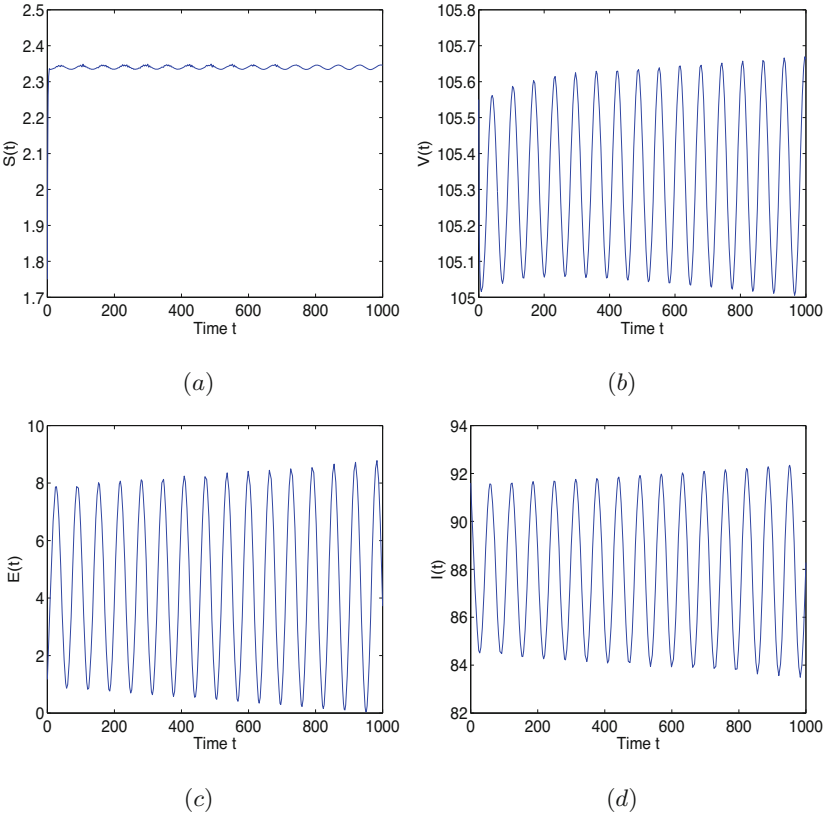


Fig. 3. The time plots for $\tau = 17.2562 > \tau_0 = 15.6626$.

For $\tau > 0$, we obtain $\upsilon_0 = 0.7195$, $\tau_0 = 15.6626$ and $\lambda'(\tau_0) = 0.009308 + i2.003327$. That is to say, the sufficient criteria for appearance of Hopf bifurcation at $\tau_0 = 15.6626$ hold. We first fix $\tau = 14.4705 \in (\tau_0 = 15.6626)$, it can be illustrated in Figs. 1–2 that the model system (28) is locally asymptotically stable. By contrary, when we fix $\tau = 17.2562 > \tau_0 = 15.6626$, them model system (28) loses its stability. Numerical simulation figures are shown as in Figs. 3–4. Specially, we have $C_1(0) = -0.000604 - i0.003251$ through some complicated computations, and then we have $\Pi_0 = 0.064890 > 0$ and $\Pi_1 = -0.001208 < 0$. Therefore, in accordance with Theorem 2, we have the conclusion that the Hopf bifurcation experiences at $\tau_0 = 15.6626$ is supercritical and the bifurcating periodic solutions exhibiting around $W_*(2.3398, 105.3279, 4.3968, 87.9355)$ are stable.

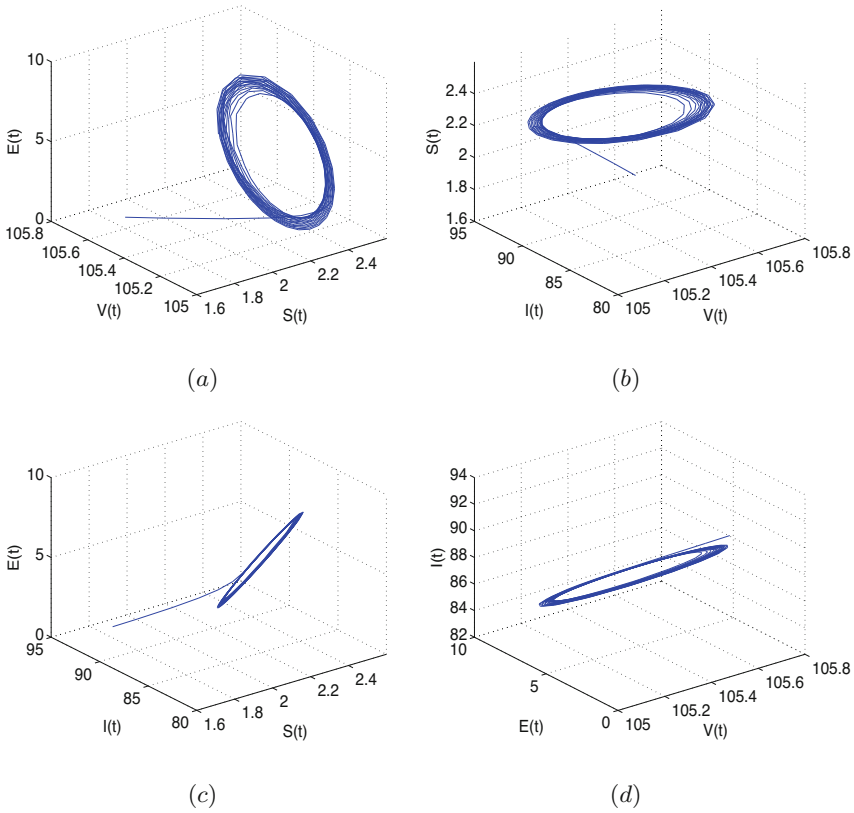


Fig. 4. The phase plots for $\tau = 17.2562 > \tau_0 = 15.6626$.

5 Conclusions

With more and more applications of networks in our daily life, the damage caused by computer viruses is also gradually obvious. Therefore, it is imperative to grope for the law governing the dissemination of computer viruses. Towards this goal, a delayed SVEIS worm propagation model concludes nonlinear incidence rate by drawing the time delay because of the incubation interval of worms into the model formulated by Upadhyay and Kumari [15]. We mainly investigate the impact of the time delay on the proposed model, and the main findings are demonstrated in the form of local stability and Hopf bifurcation.

The basic reproduction number R_0 and existence of the unique endemic equilibrium $W_*(S_*, V_*, E_*, I_*)$ are obtained. A series of sufficient criteria for local stability and exhibition of Hopf bifurcation are derived with aids of eigenvalue method. It is found that the proposed model is locally asymptotically stable when the value of the time delay is fixed below the crucial value τ_0 under some specified conditions. In this situation, the numbers of the susceptible nodes, the vaccinated nodes, the exposed nodes and the infectious nodes tend to the equi-

librium $W_*(S_*, V_*, E_*, I_*)$, and the law governing the dissemination of worms can be forecasted. Otherwise, the propagation of worms will be out of control whenever the value of the time delay exceeds the crucial value τ_0. Therefore, by taking measures to control the incubation period time delay of the worm, we can get a stable system that will be beneficial to control the spread of the worm on the network. Furthermore, direction and stability of the Hopf bifurcation are determined by center manifold method. Our study's findings supplement the work by Upadhyay and Kumari [15].

Acknowledgements. Thanks very much for your kind work on this conference. On behalf of my co-authors, we would like to express our great appreciation to editor and reviewers. We sincerely hope to get your suggestions for this paper and may this conference enjoy complete success.

References

1. Mishra, B.K., Pandey, S.K.: Dynamic model of worms with vertical transmission in computer network. Appl. Math. Comput. **217**(21), 8438–8446 (2011)
2. Feng, L.P., Song, L.P., Zhao, Q.S., Wang, H.B.: Modeling and stability analysis of worm propagation in wireless sensor network. Math. Probl. Eng. **2015**, 1–8 (2015)
3. Berghel, H.: The code red worm. Commun. ACM **44**(12), 15–19 (2001)
4. Shannon, C., Moore, D.: The spread of the witty worm. IEEE Secur. Priv. **3**(2), 46–50 (2004)
5. Hosseini, S., Azgomi, M.A., Rahmani, A.T.: Malware propagation modeling considering software diversity and immunization. J. Comput. Sci. **13**, 49–67 (2016)
6. Guillen, J.D.H., Rey, A.M.D., Encinas, L.H.: Study of the stability of a SEIRS model for computer worm propagation. Phys. A **479**, 411–421 (2017)
7. Geetha, R., Madhusudanan, V., Srinivas, M.N.: Influence of clamor on the transmission of worms in remote sensor network. Wirel. Pers. Commun. **118**(1), 461–473 (2021)
8. Xiao, X., Fu, P., Dou, C.S., Li, Q., Hu, G.W., Xia, S.T.: Design and analysis of SEIQR worm propagation model in mobile internet. Commun. Nonlinear Sci. Numer. Simul. **43**, 341–350 (2017)
9. Srivastava, P.K., Ojha, R.P., Sharma, K., Awasthi, S., Sanyal, G.: Effect of quarantine and recovery on infectious nodes in wireless sensor network. Int. J. Sens. Wirel. Commun. Control **8**, 26–36 (2018)
10. Khanh, N.H.: Dynamics of a worm propagation model with quarantine in wireless sensor networks. Appl. Math. Inf. Sci. **10**(5), 1739–1746 (2016)
11. Mishra, B.K., Keshri, N.: Mathematical model on the transmission of worms in wireless sensor network. Appl. Math. Model. **37**(6), 4103–4111 (2013)
12. Singh, A., Awasthi, A.K., Singh, K., Srivastava, P.K.: Modeling and analysis of worm propagation in wireless sensor networks. Wirel. Pers. Commun. **98**(3), 2535–2551 (2018)
13. Nwokoye, C.H., Umeh, I.I.: The SEIQR-V model: on a more accurate analytical characterization of malicious treat defense. Int. J. Inf. Technol. Comput. Sci. **9**(12), 28–37 (2017)
14. Mishra, B.K., Pandey, S.K.: Dynamic model of worm propagation in computer network. Appl. Math. Model. **38**(7), 2173–2179 (2014)

15. Upadhyay, R.K., Kumari, S.: Global stability of worm propagation model with nonlinear incidence rate in computer network. Int. J. Netw. Secur. **20**(3), 515–526 (2018)
16. Zhang, J.F.: Bifurcation analysis of a modified Holling–Tanner predator–prey model with time delay. Appl. Math. Model. **36**(3), 1219–1231 (2012)
17. Li, X.L., Wei, J.J.: On the zeros of a fourth degree exponential polynomial with applications to a neural network model with delays. Chaos, Solitons Fractals **26**(2), 519–526 (2005)
18. Hassard, B.D., Kazarinoff, N.D., Wan, Y.H.: Theory and Applications of Hopf Bifurcation. Cambridge University Press, Cambridge (1981)